BOUNDARY LAYERS AND HIGHLY SUPERSONIC MOLECULAR HYDROGEN FLOWS

J. E. Dyson

Department of Physics and Astronomy, University of Manchester, Manchester M13 9PL, England

T. W. Hartquist

Max Planck Institute for Extraterrestrial Physics, D-85740 Garching, Germany

M. T. Malone

Department of Physics and Astronomy, University of Manchester, Manchester M13 9PL, England

and

S. D. Taylor

Department of Physics and Astronomy, University College, London WC1E 6BT, England

RESUMEN

Se propone que la aceleración gradual del hidrógeno molecular en capas límites turbulentas alrededor de obstáculos (a través del acoplamiento viscoso con un viento) es responsable de los anchos de las líneas de emisión que se observan en muchas fuentes astronómicas con anchos totales a intensidad cero mayores que $100 \mathrm{~km~s}^{-1}$. En dos casos específicos, mostramos que hay una relación entre los perfiles de las líneas y las densidades de columna y que, en principio, estas dos características observacionales pueden servir como diagnóstico de estructuras de capa límite.

ABSTRACT

The gradual acceleration, through viscous coupling to a wind, of molecular hydrogen in turbulent boundary layers around obstacle clumps is proposed to be responsible for the widths of the emission features with full widths at zero intensity of greater than $100 \mathrm{~km~s}^{-1}$ seen towards many astronomical sources. We show that reasonable agreement between line profiles and column densities can be obtained for two specific cases, and that in principle, these two observational features act as diagnostics of the boundary layer structures.

Key words: **HYDRODYNAMICS — ISM: JETS AND OUTFLOWS**

1. INTRODUCTION

Practically all diffuse media encountered in astrophysics are clumpy media which are responding to the injection of energy and/or momentum. Examples range from the interaction of fast stellar winds with previously produced clumpy stellar ejecta (e.g. Dyson & Hartquist 1994) to the interaction of winds from active galactic nuclei with ejecta from nuclear stellar clusters (e.g. Perry & Dyson 1985). The most important distinction between flows initiated in clumpy, as opposed to homogeneous, media is that in the former there is mass, momentum and energy exchange at clump-flow interfaces, i.e. in boundary layers. The consequences of this exchange are major (Hartquist & Dyson 1993). The exchange reacts back on the physical, chemical and dynamical state of the global flow; conversely, the exchange is moderated by the flow.

Phenomena on three scales demand attention. The largest scale is that of the flow itself. On intermediate scales, the material ablated from clumps merges with the flow. The smallest scales involve the interfaces themselves. Observational diagnostics are of paramount importance for understanding these various phenomena.

For example, the derivation of an initial phenomenological flow model for the Wolf-Rayet nebula RCW 58 (Smith et al. 1984; Hartquist et al. 1986) was driven by UV absorption line date obtained with IUE. The flow structure in this model is radically different from that of 'classical' wind driven bubbles (Dyson 1989) and an ad hoc presentation of such a model, divorced from observational data, would have lacked justification and even credibility.

In general, clumps are embedded in global flows with systematically directed velocity fields. Thus mass ablated from clumps is accelerated in some preferred direction. Intermediate scale elongated structures or 'tails' are produced. Dyson, Hartquist, & Biro (1993) have given simple analytic and semi-analytic models of the tail shapes and, importantly, their expected appearance, which result from the various possibilities of stream-obstacle interactions. These simple models can be used to infer quite general yet robust conclusions about tail structures.

Boundary layer structures have so far received relatively less attention. Arthur, Dyson, & Hartquist (1993) constructed a spherically symmetric time-dependent numerical model to describe RCW 58. For a realistic choice of parameters, they showed that it was possible to match up the observed nebular radius, expansion velocity and—critically—the velocity spread in the gas responsible for the observed UV absorption lines. However, the temperature–velocity relationship in that model did not behave linearly, nor even monatonically, as the observational data demand. Arthur et al (1993) concluded that the resolution of this discrepancy could be obtained only if the non-equilibrium ionization structure of the flow were solved simultaneously with the hydrodynamics. For this to be possible, the effects on the flow ionization structure of material ablated in the boundary layers between clumps and flowing plasma must be incorporated. This demands an understanding of the boundary layers themselves. Smith et al (1988) had attempted to use optical emission line data to study the boundary layers, but the study was largely inconclusive.

Hartquist & Dyson (1988; 1993) noted that, in order to understand astrophysical boundary layers on other than an ad hoc basis, there existed the twin requirements of suitable spectroscopic diagnostics and spatial resolution. This latter, certainly at present, rules out the study of boundary layers in extragalactic objects. They concluded that these requirements would be best met in the context of molecular cloud phenomena. The importance of chemical diagnostics in the study of mixing phenomena is well illustrated by the chemistry of T-Tauri wind–molecular gas interactions in regions of low mass star formation discussed by Charnley et al (1990) and Nejad & Hartquist (1994).

Here we follow the same basic philosophy of using observational data to obtain semi-empirical models of boundary layer phenomena in the context of the highly supersonic H_2 motions observed in a variety of sources ranging from protoplanetary nebulae to regions of high mass star formation.

2. HIGHLY SUPERSONIC MOLECULAR HYDROGEN FLOWS

Molecular hydrogen emission profiles with widths of 100 km s^{-1} and more have been detected towards many astronomical sources (e.g. Geballe 1990). These include the Orion Becklin-Neugebauer/Kleinman-Low Nebula (e.g. Geballe et al. 1986). Perhaps most spectacular are the discrete features with centroid line-of-sight velocities spread over a range of about 250 km s^{-1} detected towards CRL 618, a protoplanetary nebula (Burton & Geballe 1990). The association with stellar objects in all these cases argues for an acceleration mechanism linked to the effects of stellar wind activity on surrounding material. The acceleration of interstellar and circumstellar material by shocks preceding stellar wind driven bubbles in fact, accounts for many observed dynamical phenomena.

Shock acceleration of molecular material to such high velocities has, however, serious difficulties. Standard hydrodynamic J-type shocks dissociate H_2 for shock velocities greater than about 25 km s^{-1}. Magnetically moderated C-type shocks dissociate H_2 at shock speeds in excess of about 50 km s^{-1} if they propagate into dense material with standard pre-shock magnetosonic speeds (Draine, Roberge, & Dalgarno 1983; McKee, Chernoff, & Hollenbach 1984). Moreover, standard C-type shocks cannot produce the high excitation H_2 emission observed in OMC-1 (Moorhouse et al. 1990). Chernoff, Hollenbach, & McKee (1982) speculated that the broad H_2 profile wings originate in a molecular reformation region in an initially molecular stellar wind which has passed through an inner dissociating shock in a wind-blown bubble. Dalgarno (1993) pointed out that spatially coincident emissions from SO and SO$^+$ might, if observed, indicate the existence of such a dissociating shock. Smith, Brand, & Moorhouse (1991) have noted that the inner shock in the wind would not be dissociating if the magnetosonic speed in the preshock wind were high enough. However, the origin of the high magnetic fields needed is problematic and is an ad hoc assumption of the Smith et al (1991) model. The problems of shock acceleration and attempts to circumvent them have recently been reviewed by Brand (1995).

Hartquist & Dyson (1987) pointed out that, in principle, H_2 can reach very high velocities without suffering

dissociation if it is contained in the shell of a wind-blown bubble which is expanding into an ambient medium with a density decreasing more rapidly than the wind diverges. For example, this occurs when a spherically symmetric steady wind expands into a spherically symmetric ambient medium which has a power law density distribution falling off more rapidly than an inverse square dependence with distance from the wind source. Other density distributions (e.g. exponential) also admit shell acceleration once the shell has travelled roughly a density scale-height away from the wind source. The key element in the Hartquist & Dyson (1987) model is that swept-up molecular gas passes through a sonic point and is accelerated to velocities supersonic with respect to the ambient material whilst the shell (i.e. the shock heading it) is moving at a velocity less than that of a dissociating shock. Further, subsequent shell acceleration occurs so gradually that the gas never heats up sufficiently for it to make a subsequent supersonic to subsonic transition or for the molecules in it to be dissociated. This model has attractive features. The accelerated molecule-bearing shell may fragment by Rayleigh-Taylor instability, though for high density contrast clumps to form, fast enough shocks ($\gtrsim$ 100 km s^{-1}) to generate genuine thermal instability in the post-shock gas are probably required (Hartquist & Dyson 1987). Fragmentation would naturally produce fast discrete H$_2$ features.

We here develop a rather different picture first described by Malone, Dyson & Hartquist (1994) for the acceleration of H$_2$ to high velocities but retain several key elements of the above model. We investigate the structures of flows in boundary layers between fast winds and embedded clumps. Acceleration of gas that has become supersonic at temperatures low compared to those required for molecular dissociation is continuous as the gas flows along a boundary layer. In Section 3 we describe the basic features of a two dimensional steady model of a boundary layer. In Section 4 we give a simple isothermal model and apply it to the Orion BN/KL region. In Section 5 we describe models incorporating heating and cooling and simple chemistry. In Section 6 we discuss advantages of the boundary layer model and outline future work in this area.

3. THE BASIC MODEL OF FLOW IN A STEADY STATE BOUNDARY LAYER

We assume that clumps are embedded in a protostellar wind; that the wind drives a converging shock through the clumps (but does not destroy them); that, following shock passage, the shocked clump gas cools quickly; finally, that the magnetic pressure greatly exceeds the thermal pressure in the final clump configuration. A boundary layer whose thickness will be a few per cent or so of the clump linear extent is set up (Hartquist & Dyson 1988). Since the wind is hypersonic, the magnetic field will be essentially parallel to the boundary layer. The variables x and z respectively measure distance along the boundary layer and height perpendicular to the inner edge of the boundary layer. Since the layer is thin, $\partial P/\partial z = 0$, where $P(= P_T + P_M)$ is the total pressure (i.e. the sum of the thermal pressure P_T and the magnetic pressure P_M). The wind adds mass, energy and momentum to the boundary layer. In general, the deposition rates of these quantities are functions of x and z. An essential aim of this model is to determine these deposition rates by comparison of the model with the observational data.

The continuity equation for the flow of ablated cloud material and mixed-in wind gas in the layer is

$$\frac{\partial}{\partial x}(\rho v_x) + \frac{\partial}{\partial z}(\rho v_z) = S \tag{1}$$

where ρ is the density, $\underline{v}(\equiv v_x \hat{x} + v_z \hat{z})$ is the fluid velocity, and $\hat{x}$ and $\hat{z}$ are unit vectors in the x and z directions respectively. S is the volume deposition rate of mass into the boundary layer from the wind.

The momentum equation is

$$\frac{\partial}{\partial x}(\rho v_x \underline{v}) + \frac{\partial}{\partial z}(\rho v_z \underline{v}) + \hat{x}\frac{\partial P}{\partial x} = \hat{x}F_x \tag{2}$$

where $\hat{x}F_x$ is the volume force exerted on the flow in the boundary layer through its coupling to the wind. The coupling can be due either to the direct mixing of wind material or to the propagation and dissipation of waves generated by the response of the wind to its encounter with the clump.

The energy equation is

$$\frac{\partial}{\partial x}\left(\frac{1}{2}\rho v_x v^2 + v_x \sum n_p U_p\right) + \frac{\partial}{\partial z}\left(\frac{1}{2}\rho v_z v^2 + v_z \sum n_p U_p\right) = -v_x\frac{\partial P}{\partial x} + \mathcal{H} - \Lambda \tag{3}$$

where $\mathcal{H}$ and Λ are respectively the volume energy injection rate and the volume cooling rate; n_p and U_p are respectively the number density and internal energy per particle of particle p. We consider only contributions

from H and H_2 to the internal energy term. The cooling rate Λ includes cooling from a variety of sources (H_2, CO, H_2O, etc.) and supplementary conservation equations (analogous to (1)) are required for each species.
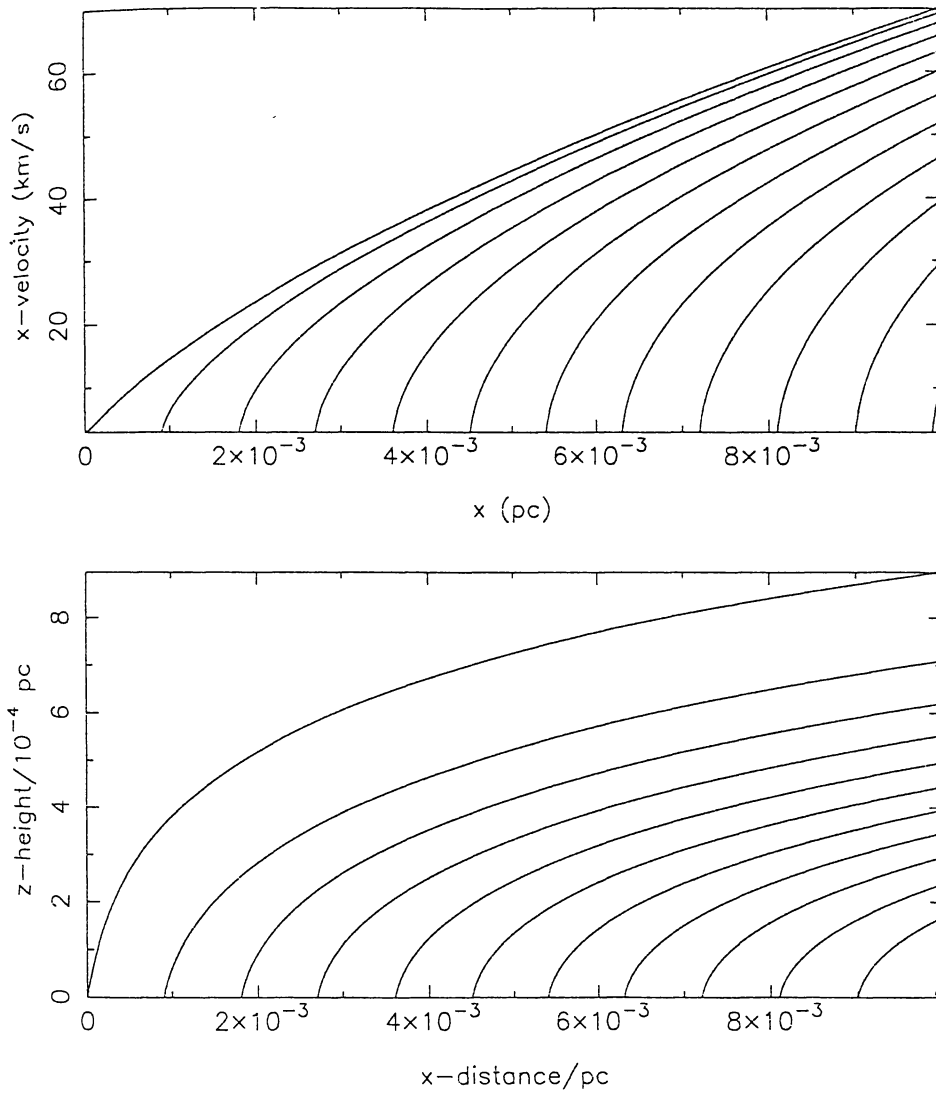

Fig. 1.— The flow in an isothermal BN/KL boundary Layer. The model parameters are as in the text. The upper and lower frames show the velocity and the height of a trajectory above the base of the boundary layer.

To solve (1) and (2), we follow the flow along each of a number of trajectories starting at $x = x_i$, $z = 0$, where x_i is the starting point of the ith trajectory along which z is taken to be a function of z. Thus

$$z = \int_{x_i}^{x} (v_z/v_x)\,dx \qquad (4)$$

$$\frac{dv_x}{dx} = \frac{1}{\rho v_x}\left[f_x - Sv_x - \frac{dP}{dx}\right] \qquad (5)$$

$$\frac{dv_z}{dx} = -\frac{v_z}{v_x}\frac{S}{\rho} \qquad (6)$$

where we have used (1) and (2) and written $\partial/\partial z \equiv (v_x/v_z)(d/dx - \partial/\partial x)$. Analogous equations can be written for other derivatives, e.g. dT/dx, $d\rho/dx$, etc. We need also to specify P as a function of x. Since the magnetic field is nearly parallel to the boundary layer we can write

$$\frac{dP}{dx} = \frac{dP_T}{dx}. \tag{7}$$

To fix the pressure variation, we assume that a bow shock with a given shape lies between the wind and the boundary layer. We take the shape to be given by $z = \alpha x^{1/2}$ where α is a constant which fixes both the variation of P along the layer and the pressure drop from the front of the cloud to its back. This particular choice corresponds to the shock shape used by Smith et al (1991). Across this shock, the normal velocity component of the wind is thermalized, and this gives the prescription for $P(x)$. The magnetic pressure effectively balances the normal component of the momentum flux whilst momentum input to the boundary layer comes from the tangential component of this flux. We then specify

$$P_T \equiv \beta P = \frac{\beta \alpha^2 \rho_\omega v_\omega^2}{\alpha^2 + 4x} \tag{8}$$

$$S = \frac{\alpha \rho_\omega v_\omega}{(\alpha^2 + 4x)L} \left(\frac{d}{\delta}\right) f(z) \tag{9}$$

$$F_x = \frac{2\alpha x^{1/2} \rho_\omega v_\omega^2}{(\alpha^2 + 4x)L} \left(\frac{d}{\delta}\right) g(z) \tag{10}$$

$$\mathcal{H} = \frac{1}{2} \frac{\alpha \rho_\omega v_\omega^3}{(\alpha^2 + 4z)^{1/2}L} \left(\frac{d}{\delta}\right) h(z). \tag{11}$$

These source terms are appropriate if direct mixing of stellar wind gas into the boundary layer only is considered. In these equations, δ is the boundary layer thickness and d^2 the cross-sectional area presented by the clump to a wind with pre-shock density and velocity ρ_ω and v_ω respectively. The clump length is L. The functions f, g and h describe the z dependences of the deposition rates which are to be prescribed and equal unity for constant (with respect to z) rates. We everywhere take $d/\delta \approx 10$ (cf. Hartquist & Dyson 1988).

4. AN ISOTHERMAL BOUNDARY LAYER FOR THE BN/KL REGION

Here we replace the energy equation (3) by $T = T_0$ and hence $\rho = \mu P_T/k_B T_0$, where k_B is Boltzmann's constant and μ the mean mass per particle in the boundary layer. We use a suggested stellar mass loss rate $\dot{M}_* = 8.8\,10^{-4}\,M_\odot\,\mathrm{yr}^{-1}$ for IRc 2 (Chernoff et al. 1982; Levreault 1988) and a wind velocity $v_\omega = 200\,\mathrm{km\,s}^{-1}$ which give $\rho_\omega = 10^{-20}\,\mathrm{gm\,cm}^{-3}$ if the wind source is situated at a distance $D = 0.05\mathrm{pc}$ from the clump. The choices for T_0, β and L are respectively 2000K, 0.1 and 0.01 pc. We use a value of α such that the pressure drops by a factor of 10 from one end of the clump to the other.

Figure 1 shows the velocity v_x and height z as functions of x for several particle trajectories. The maximum flow speed reached is about 70 km s^{-1} which is encouragingly close to the half-widths at zero intensity of the BN/KL H$_2$ emission features. With this set of parameters, the cloud magnetic field is 10 mG at $x = 0$ and drops to 3 mG at $x = L$. Over the same spatial interval, the H$_2$ number density varies from about 9 10^5 cm^{-3} to 9 10^4 cm^{-3} for a ratio of He to H$_2$ number density of 1:8. The choice of $T_0 = 2000$ K is consistent with a typical heating rate $\mathcal{H} \simeq (\rho_\omega v_\omega^3/L)(d/\delta)$ and a thermal equilibrium cooling rate at 2000 K of about 5 10^{-20} erg s^{-1} per H$_2$ molecule (Hartquist, Oppenheimer, & Dalgarno 1980). We note, however, that the observed line intensity ratios clearly show that the emitting gas cannot be isothermal (Brand et al. 1988).

To calculate characteristic line profiles, we assume that the Orion BN/KL region contains many clumps (e.g. Brand et al. 1989). An H$_2$ line profile has contributions from boundary layers around each clump. We then assume that the emissivity of a particular gas element in the boundary layer is directly proportional to its mass and is independent of all other parameters except, of course, its velocity, which determines the emission frequency. Fig. 2 shows the normalized intensity as a function of velocity of a feature produced by the boundary layers of 32 clumps distributed in a plane at equal angular intervals. The observer and wind source lie in the

same plane and a clump lies directly between the wind source and the observer. We adopt this configuration as standard. Thermal broadening of 3 km s^{-1} is assumed in each parcel of gas and a Gaussian instrumental broadening of 16 km s^{-1} included. It is encouraging that such a very simple model gives a reasonable fit to typical BN/KL line profiles.
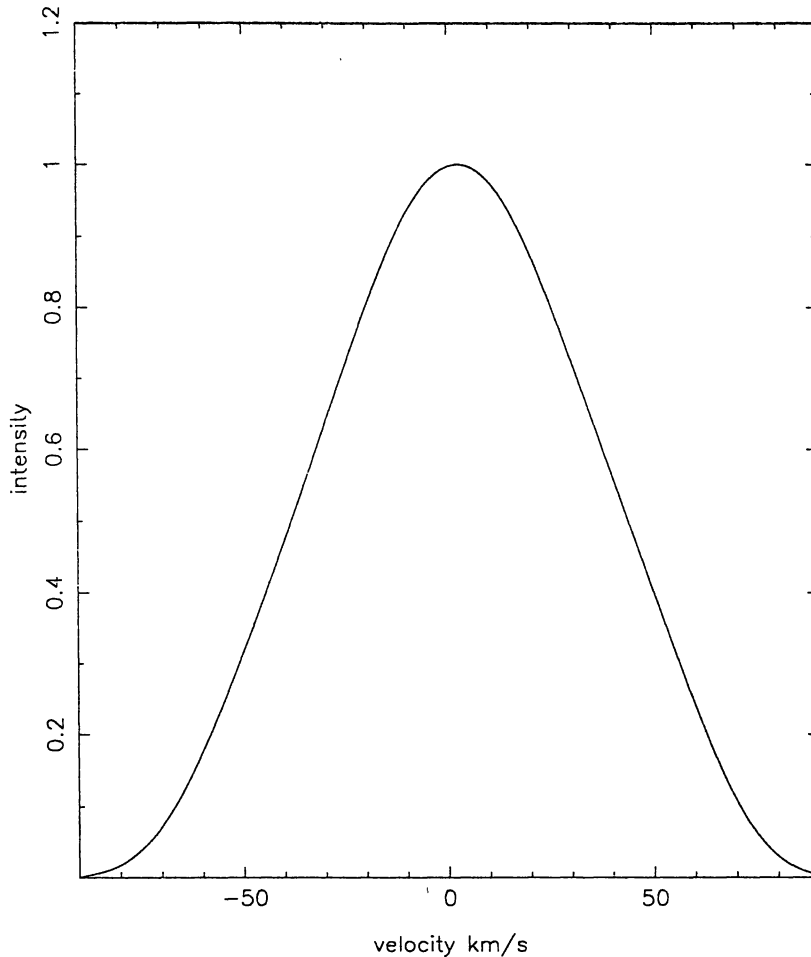

Fig. 2.— A line profile calculated from the contribution of many boundary layers distributed evenly around the source of a spherically symmetric wind using the BN/KL parameters.

5.   BOUNDARY LAYER MODELS INCLUDING HEATING AND COOLING

We now consider solutions to (1)–(3) and initially assume no z dependence of the deposition rates. The clump gas has assumed initial small abundances of O, O_2, H_2O and OH. Seventeen reactions involving these species together with H and H_2 are included (Malone 1995). The base velocity of the clump gas is taken as the sound speed in gas at 10 K ($v_x(z = 0) = 0.2$ km s^{-1}). We keep the same values of L and D as above. We further adopt $\dot{M}_* = 1.1\ 10^{-3} M_\odot$ yr^{-1}, $v_\omega = 300$ km s^{-1} and $\beta = 0.025$. The pressure drops along the clump by a factor of 6. Figure 3 shows v_x and z as a function of x for a set of trajectories. Clearly, the boundary layer is rather thicker than in the isothermal case due to an increased temperature which reaches a maximum value close to 3000 K. At this peak temperature, the boundary layer has a number density of about 10^5 cm^{-3}, about half of which is in the form of H_2. The maximum velocity obtained is about 10 km s^{-1} greater than in the isothermal case.

In Fig. 4 we compare column densities (or line intensities) calculated for this boundary layer with those given by Brand et al (1988). They are normalized to the intensity of the $v = 1 \rightarrow 0S(1)$ transition. The fit is
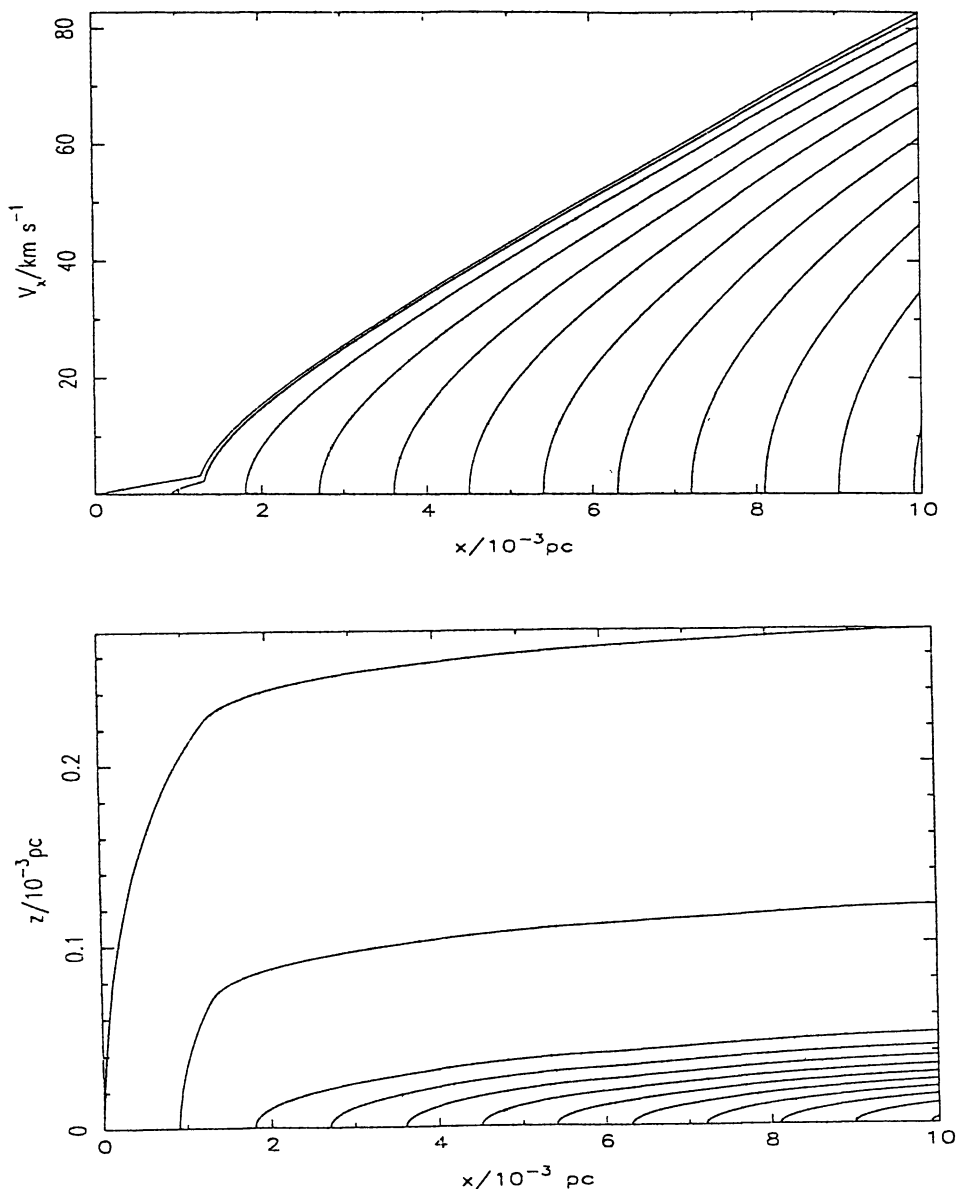
Fig. 3.— The flow in a boundary layer calculated with constant heating and momentum input rates and with molecular cooling. The upper and lower frames show respectively the velocity component parallel to the boundary layer and the height above the boundary layer base.

satisfactory considering the simplicity of the model, but the fit gets progressively worse at higher line excitation energies. We also find that the calculated line profiles do not agree well with those observed in two important respects. Firstly, lines with excitation temperatures $\gtrsim$ 13000 K develop non-observed secondary symmetric shoulders in their profiles, which arise from the hottest gas. Secondly, there are significant differences in line widths for lines of differing excitation temperatures. The observational data show that differences are in fact small. Increasing the energy deposition rate partially removes the secondary shoulders since at the increased peak temperature in the layer which results, H_2 is removed. However, for lines at higher excitation energies, the calculated column densities show even more deviation from those observed. The column density fit at higher excitation energies is quite critically dependent on the pressure drop along the cloud.

Much better line profile fits are obtained if the deposition rates are assumed to have a simple linear dependence on z. But again significant difficulty is found in obtaining column densities of high excitation lines in agreement with the observational data. What is evident from our investigations so far is that models where the temperature of the ablated mixture rises rapidly and then cools, and where momentum injection is concentrated towards the rear of the cloud, seem to fit the data best.
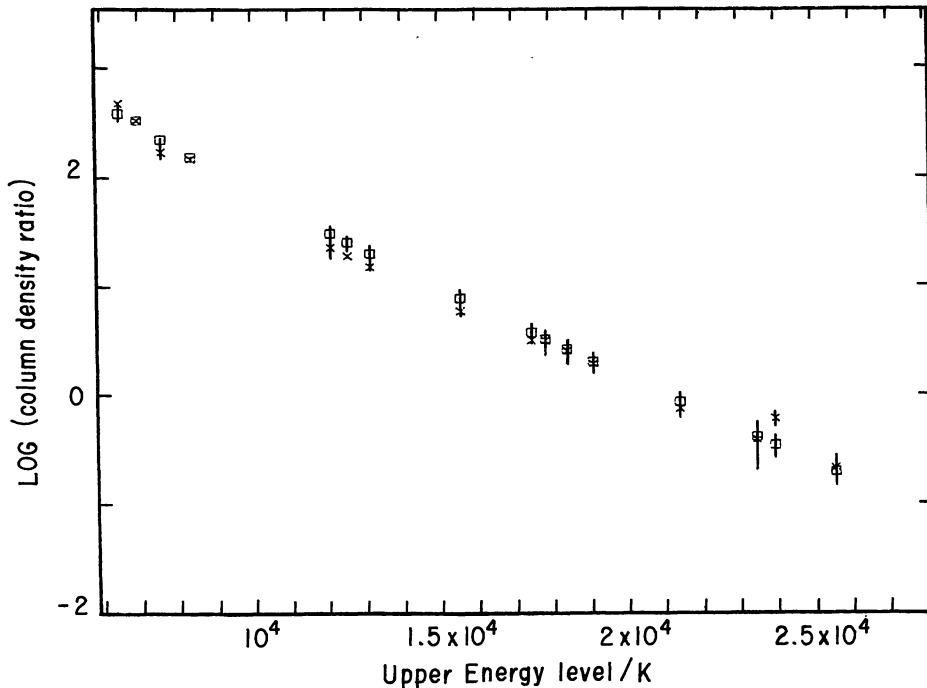

Fig. 4.— Comparison of observed (crosses) and calculated (boxes) column densities for lines of different excitation energy using the non-isothermal boundary layer discussed in the text.

6. DISCUSSION AND CONCLUSIONS

The model presented has some appreciable advantages over shock acceleration models. The acceleration in the boundary layer is sustained along its entire length by viscous coupling between the fast wind and the clump gas. The viscous coupling arises due to the presence of shear induced turbulence (e.g. Hartquist & Dyson 1988) and the damping of waves associated with it. That this acceleration is gradual and sustained means that the molecules ablated from the clump are not dissociated whilst reaching high speeds.

Clumps must have quite high magnetic fields which we argue arise naturally by the winds' driving shocks through clumps, thereby bringing the magnetic pressure in each into approximate balance with the wind ram pressure. Unlike the Smith et al. (1991) model, there is no need to make the ad hoc assumption that such high fields exist. Although shocks driven into the clumps may be dissociating, post-shock H_2 reformation can occur provided the clumps are dense and large enough.

It is clear that considerable further work needs to be done on this model in (at least) two important areas. Firstly, examination of various functional forms for the spatial variation of the deposition rates is necessary. A start has been made as noted in Section 5. Further, sensible line profile calculations demand a more realistic model for the spatial distribution of clumps which presumably is linked to the global flows occurring in the regions studied.

One of us (JED) is grateful to the organizers of this meeting for their kind invitation to present this work in the tropical paradise in which it took place.

REFERENCES

Arthur, S. J., Dyson, J. E. & Hartquist, T. W. 1993, MNRAS, 261, 425
Brand, P. W. J. L. 1995, in Circumstellar Matter, ed. G. D. Watt & P. M. Williams, in press
Brand, P. W. J. L., Burton, M. G., Geballe, T. R., Moorhouse, A., Bird, M., & Wade, R. D. 1988, ApJ, 334, L103
Brand, P. W. J. L., Toner, M. P., Geballe, T. R., & Webster, A. S. 1989, MNRAS, 237, 1009
Burton, M. G., & Geballe, T. R. 1986, MNRAS, 223, 13p
Charnley, S. B., Dyson, J. E., Hartquist, T. W., & Williams, D. A. 1990, MNRAS, 243, 405
Chernoff, D. F., Hollenbach, D. J., & McKee, C. F. 1982, ApJ, 259, L97
Dalgarno, A. 1993, JRoySocChem: Faraday Transactions, 89, 2111
Draine, B. T., Roberge, W. G., & Dalgarno, A. 1983, ApJ, 264, 485
Dyson, J. E. 1989, in Structure and Dynamics of the Interstellar Medium, IAU Colloquium 121, ed. G. Tenorio-Tagle, M. Moles, & J. Melnick (Springer Verlag), 149
Dyson, J. E., & Hartquist, T. W. 1994, in Circumstellar Media in the Late Stages of Stellar Evolution, ed. R. E. S. Clegg, I. R. Stevens, & W. P. S. Meikle (Cambridge University Press), 52
Dyson, J. E., Hartquist, T. W., & Biro, S. 1993, MNRAS, 261, 430
Geballe, T. R. 1990, in Molecular Astrophysics—A Volume Honouring Alexander Dalgarno, ed. T. W. Hartquist (Cambridge University Press), 345
Geballe, T. R., Persson, S. E., Simon, T., Lonsdale, C. J., & McGregor, P. J. 1986, ApJ, 302, 500
Hartquist, T. W., & Dyson, J. E. 1987, MNRAS, 228, 957
Hartquist, T. W., & Dyson, J. E. 1988, Ap&SS, 144, 615
Hartquist, T. W., & Dyson, J. E. 1993, QJRAS, 34, 57
Hartquist, T. W., Dyson, J. E., Pettini, M., & Smith, L. J. 1986, MNRAS, 221, 715
Hartquist, T. W., Oppenheimer, M., & Dalgarno, A. 1980, ApJ, 236, 182
Levreault, R. M. 1988, ApJ, 330, 897
Malone, M. T. 1995, PhD Thesis, Victoria University of Manchester, in preparation
Malone, M. T., Dyson, J. E., & Hartquist, T. W. 1994, Ap&SS, 216, 143
McKee, C. F., Chernoff, D. F., & Hollenbach, D. J. 1984, in Galactic and Extragalactic Infrared Spectroscopy, ed. M. F. Kessler & J. P. Phillips (Reidel Publ. Co., Dordrecht), 103
Moorhouse, A., Brand, P. W. J. L., Geballe, T. R., & Burton, M. G. 1990, MNRAS, 242, 88
Nejad, L. A. M., & Hartquist, T. W. 1994, Ap&SS, 220, 253
Perry, J. J., & Dyson, J. E. 1985, MNRAS, 213, 665
Smith, L. J., Pettini, M., Dyson, J. E., & Hartquist, T. W. 1984, MNRAS, 211, 697
Smith, L. J., Pettini, M., Dyson, J. E., & Hartquist, T. W. 1988, MNRAS, 234, 625
Smith, M. D., Brand, P. W. J. L., & Moorhouse, A. 1991, MNRAS, 248, 730